Chapter 6
In-vitro cell line studies

6 In-vitro cell line studies

6.1 Introduction

Cell line may be defined as cells that are derived from identical parental cells having uniform genetic makeup, which can proliferate indefinitely in laboratory when introduced in culture media [1]. Cell lines are broadly classified into two types – (i) Finite cell line which have limited life span and can undergo fixed number of passages after which their growth rate declines (ii) Continuous cell lines are immortalized cells which have unlimited life and can grow faster. Furthermore, cell line may either be adherent type culture or suspension culture based on property of constituent cell to adhere to surface. The cells used in preparing cell-lines, based on morphology, can be divided into three categories – fibroblastic cells (elongated shape), epithelial like cells (polygonal shape) and lymphoblast like cells (spherical shape).

These cell lines have wide application in research for drug development studies like drug metabolism and cytotoxicity, vaccine production, study of gene function, antibody production, artificial tissues generation and manufacturing of biological compounds [2-4]. Presently, cell lines have become popular as they offer several benefits like ease of use, unlimited supply, no ethical concerns as faced during use of animal or human tissues and cost effectiveness. This can be evidenced as till now over 3600 cell lines from more than 150 species have been developed and utilized [5]. Still, there are some concerns which may be faced while using cell lines like alteration of phenotype due to genetic manipulation, genetic and phenotypic variation over time, genetic drift causing heterogenicity, contamination and cross-contamination issues etc. Thus, proper measures and great care must be taken while concluding any research findings from cell line studies along with supporting evidences from other studies.

6.2 SK-N-MC cell line

Organism:	Homo sapiens, human
Tissue:	Brain; derived from metastatic site: supra-orbital area
Disease:	Neuroepithelioma
Morphology:	Epithelial
Derivation:	Neurogenic origin derived by J.L. Biedler. and was isolated in September of 1971.

Complete growth medium:	Minimum essential medium (MEM with sodium pyruvate) supplemented with 10% FCS and 1% antibiotic-antimycotic solution
Subcultivation ratio:	1:6 to 1:12
Media renewal:	2-3 times per week
Culture conditions:	Atmosphere: Air (95%); carbon dioxide (5%) Temperature: 37 ^{0}C

6.3 Subculturing/ passaging

6.3.1 Background

It involves transfer of cells to fresh media after removal of previous media which ensures further propagation of cells. In adherent cell lines when cells occupy complete surface or when they exceed capacity of complete media to support growth, subculturing is to be done to stimulate continuous growth. The factors that decides schedule of subculturing includes growth phase of cells i.e. passaging should be done in log phase of cells before reaching confluence and pH of growth media (drop in pH due to lactic acid accumulation entails subculturing).

6.3.2 Protocol

- The used culture media was discarded from the tissue culture flask.
- The cells were washed properly by adding PBS (pH 7.4) and the flask was rocked back and forth to remove traces of media which might interfere with dissociating reagent.
- After discarding PBS, 2 ml trypsin-EDTA per flask (25 cm^2 surface area) was added such that entire cell surface was covered with dissociating medium.
- The flask was gently tapped to detach cells attached to surface and incubated for 2 min.
- Later, after achieving satisfactory cell dissociation, which was confirmed by observing through microscope, 4 ml complete media was added to neutralize dissociating reagent and mixed well.
- The cell suspension was transferred to microcentrifuge tubes and centrifuged at 2000 rpm for 5 min. Later, the supernatant was discarded and cell pellet was resuspended in fresh complete media.

- The cell suspension was diluted properly and according to subculturing ratio, fixed volume of cell suspension was added to tissue culture flask along with fresh complete media which was then placed in incubator.

6.4 Cell counting

6.4.1 Protocol

- The coverslip and hemocytometer were cleaned with 70% isopropyl alcohol and air dried. Dry coverslip was placed in position in hemocytometer.
- Using dissociation reagent cells were trypsinized and detached from culture flasks.
- Suitable volume of cell suspension was mixed with equal volume of 0.4% trypan blue in PBS. Trypan blue exclusion test was performed to exclude non-viable cells which were stained blue in presence of trypan blue.
- This cell suspension mixture was added to hemocytometer and observed under microscope (10x).
- Cells were counted in 5 squares as shown in Figure 6. 1 and average cells per square was calculated.

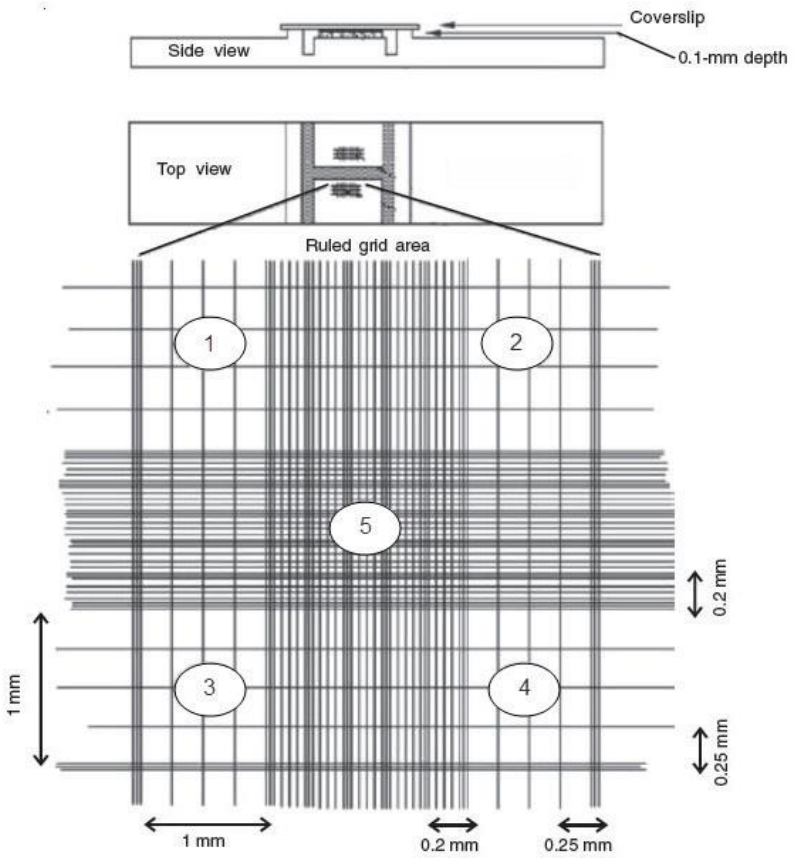

Figure 6. 1: Representation of cell counting areas using hemocytometer

- Total cells per ml was calculated from average cells using following formula

$$Total\ cells = Average\ cells\ per\ square \times dilution\ factor \times 10^4$$

6.5 Cell cytotoxicity study

6.5.1 Background

Cell cytotoxicity assay deals with quantitative and sensitive estimation of growth rate of cells to measure cell proliferation. This assay has wide application in testing action of drugs, cytotoxic compounds and screening of biologically active compounds. The main techniques to estimate cell cytotoxicity includes employment of formazan dyes, protease biomarkers or estimating ATP content. Additionally, cell cytotoxicity can also be measured by SRB and WST-1 assays. Currently, application of formazan dyes including INT, MTT, MTS and XTT is widely employed for cytotoxicity estimation. Amongst all the procedures, MTT assay, conceptualized by Mossman [6], is considered as popular and versatile protocol for estimating cytotoxicity. MTT (3-(4, 5-dimethylthiazolyl-2)-2,5-diphenyltetrazolium bromide) assay principally works on conversion of tetrazolium salt into insoluble formazan crystals [7-10]. Generally, in metabolically active cells, under influence of mitochondrial and oxidoreductase enzymatic action, reduction of yellow colored MTT tetrazolium salt occurs to purple colored formazan crystals. These formazan crystals are solubilized using suitable solvent like DMSO and resulting colored solution can be estimated spectrophotometrically at 570 nm [11].

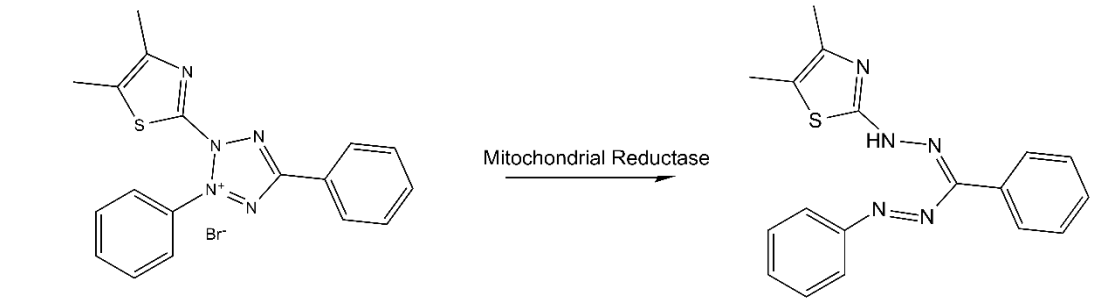

3-(4,5-dimethylthiazol-2-yl)-2,5-diphenyltetrazolium bromide **(MTT)**

(*E*,*Z*)-5-(4,5-dimethylthiazol-2-yl)-1,3-diphenylformazan **(Formazan)**

Figure 6. 2: Principle of MTT assay

6.5.2 Protocol

- The adherent cells were trypsinized and detached from tissue culture flask, resultant cell suspension was diluted suitably to achieve cell concentration of 5×10^3 cells per 200 µl.

- 200 µl stock cell suspension was pipetted out in each well of 96 well plate and the resulting well plate was incubated for 24 h in CO_2 incubator to allow cells to adhere surface of well plate.
- After 24 h, old media was discarded and cells were treated with synthesized copolymers and conjugates dissolved in complete media (MEM with sodium pyruvate + 10% FCS + 1% antibiotic-antimycotic solution) and suitably diluted to achieve desired concentration. Additionally, treatment with saline was employed in triplicate to be used as control.
- Such treated cells were incubated in incubator for 24 h after which the polymeric solution was replaced with fresh media.
- Subsequently, 20 µl MTT solution (5mg/ml) was added to each well and incubated for 4-6 h.
- After incubation, the contents from well were discarded and immediately 200 µl DMSO was added to each well to dissolve formazan crystals.
- The reduction of viable cells was determined immediately by colorimetry at 570 nm (keeping reference filter of 655 nm) using an Enzyme-Linked Immune Sorbent Assay (ELISA) plate reader.
- Cell viability of each group was expressed as a relative percentage to that of control cells [12, 13] and percent cell viability of each well was determined using following equation

$$\%\ cell\ viability\ = \frac{OD(sample)}{OD(control)} \times 100$$

6.6 In-vitro permeation study

6.6.1 Background

Brain delivery of therapeutics faces several barriers when administered in-vivo and thus to bypass those barriers nose to brain delivery was proposed. Although, this route doesn't pose BBB and other similar barriers, some factors including nasal enzymes, nasal mucosa, epithelium and muco-ciliary clearance have important role in limiting permeability of therapeutics via. nasal route. Thus, it is important to assess permeability across nasal mucosa to determine brain delivery capacity of administered therapeutics. Various techniques are available for determining drug permeability across epithelium, amongst which animal tests are considered as gold standard. Still, it has certain constraints as these techniques are time consuming, expensive and cannot simulate human conditions perfectly. Thus, in-vitro cell culture models which offers

rapid, cost-effective and adequate predictability have been considered as better alternative to in-vivo studies. Additionally, parameters and experimental conditions during in-vitro testing can be strictly regulated and use of human cell lines avoids predictability and ethical issues arising due to use of animal tissues [14]. Amongst all the available techniques, Transwell® is most widely used cell culture technique for drug permeability study. Transwell® support can be made either from polycarbonate, polyester or polytetrafluoroethylene which affects membrane characteristics like optical properties, cell visibility etc. Along with permeation, Transwell® also has important application in study of cellular functions like transport, secretion etc.

6.6.2 Protocol

- The adherent cells were trypsinized and detached from tissue culture flask, and seeded at density of 1×10^6 cells/insert in Transwell®.
- The stock cell suspension was diluted such that desired cell concentration is achieved in 500 µl complete media. This was then added from apical surface of pre-wet transwell® inserts and 1.5 ml complete media was added in basolateral chamber. This was incubated in CO_2 incubator at 37 °C and media was changed every 24 h.
- The monolayer integrity of cells was checked regularly by measuring transepithelial electrical resistance (TEER) using Millicel-ERS-2 Voltohmmeter (Millipore, USA) and permeability assay was commenced after 9-12 days when TEER value above 170 $\Omega.cm^2$ was obtained.
- Before starting, media was removed and transport media (HBSS + 25 mM HEPES + 0.35 g/l $NaHCO_3$) was added to both apical and basolateral chamber and the plate was allowed to equilibrate for 1 h at 37 °C in CO_2 incubator.
- Subsequently, fluorescently labelled formulations diluted in 0.5 ml transport media were added to apical chamber of inserts and plate was incubated at 37 °C at 500 rpm in orbital shaker.
- 20 µl sample was withdrawn from basolateral chamber at 0, 15, 30, 60, 90 and 120 min and replaced with equal volume of fresh transport media. Additionally, sample was withdrawn form apical chamber at initial and final time points.
- The samples were analyzed by fluorimetry to determine amount of fluorescently tagged formulation transported to receptor compartment
- Apparent permeability coefficient was calculated from the following equation

$$P_{app} = \frac{dQ}{dt} \times \frac{1}{A \times C_o}$$

Where,

P_{app} = apparent permeability coefficient

$\frac{dQ}{dt}$ = cumulative flux (slope of cumulative transported amount w.r.t. time)

A =surface area of inserts (1.13 cm^2 in 12 well plate)

C_o = initial concentration on apical side

6.7 Cell uptake study

For cellular uptake study, cyanine5 labelled siRNA negative control was employed. Qualitative uptake and intracellular accumulation was determined using confocal microscopy while quantitative cell uptake was determined by flow cytometry.

6.7.1 Confocal microscopy

6.7.1.1 Background

Confocal microscopy is currently most widely used technique to visualize cellular uptake of fluorescently labelled formulation administered. Although, this technique provides only qualitative information, it is still preferred technique to determine cellular uptake as transfection efficiency of different formulations can be compared along with their intracellular localization. This technique employs optical sectioning which allows depth selection while capturing images and thus removes artifacts occurring during sectioning and staining evident in conventional fluorescent microscope. Optical sectioning, which produces specimen section using light, can be achieved by deconvolution and multiphoton imaging. This microscope employs argon, krypton and helium-neon laser as light source and photomultiplier tubes behind pinholes as detectors. The main upper edge using this technique is high resolution of resulting image as information from different depth of specimen is not superimposed. Additionally, background information retrieval can be controlled and thus image degradation can be avoided. Thus, removal of background fluorescence along with better signal to noise ratio produces highly resolving image. While employing confocal microscope care must be taken to avoid artifact production due to either of three processes like bleed through phenomenon (crossover or crosstalk), photobleaching and autofluorescence [15-17].

6.7.1.2 Protocol

- The adherent cells were trypsinized and detached from tissue culture flask, resultant cell suspension was diluted suitably to achieve cell concentration of 10^4 cells per 100 µl.
- 100 µl of stock cell suspension was pipetted out in each well of 6 well plate with glass coverslips at the bottom.
- The resulting well plate was incubated for 24 h in CO_2 incubator for proper adherence of cells to glass coverslips.
- After incubation, old media was carefully pipetted out without disturbing adhered cells and subsequently, 100 µl fluorescently labelled polyplexes or lipopolyplexes (Cy5-siRNA conjugated formulations) diluted in complete media was added.
- The resulting plate was incubated for 6 h protected from light in CO_2 incubator and after incubation, cells were washed three times with ice cold PBS.
- Subsequently, cells were fixed by their incubation with 4% paraformaldehyde solution for 10 min.
- Later, nuclei staining was performed by incubating cells with 1 µM DAPI solution for 10 min. The cells were washed again three times with ice cold PBS to remove background fluorescence.
- Such treated coverslips were mounted on slides using 70% glycerol as a mounting reagent and proceeded for confocal microscopy using confocal laser scanning microscope (LSM 710, Carl-Zeiss Inc., USA).

6.7.2 Flow cytometry

6.7.2.1 Background

Flow cytometry is innovative technique which provides determination of quantitative cellular uptake of fluorescently labelled gene therapeutic carriers and other formulations. This technique allows counting cells, determination of physico-chemical characteristics of cells and sort heterogenous cell population i.e. suspended in fluid stream. The instrumentation is composed of five basic subunits – (i) flow cell which carries and aligns cells in unilamellar fluid stream (ii) measuring system (iii) detector having capability to detect fluorescence (iv) amplification system (v) computer for data processing. The principle involves measuring fluorescence and light scattering due to particle or cell passing through laser beam providing uniform intensity and focused on

sample fluid stream. Scattered light (forward scatter) can provide particulate information like size, surface characteristics etc. while fluorescence intensity (side scatter) can provide variety of information depending on the aim of study. Flow cytometry can be employed for variety of applications including enzyme activity, measurement of nucleic acid content, calcium flow, intracellular pH and membrane potential. Fluorescence activated cell sorting (FACS) is specialized type of flow cytometry technique which can sort heterogenous cell population based on their characteristics and thus has wide application to determine penetration and transfection efficiency of different formulations along with their cellular uptake [15, 18-20].

6.7.2.2 Protocol

- The adherent cells were trypsinized and detached from tissue culture flask, and seeded in each well of 6 well plate with cell density of 1×10^6 cells/well.
- After incubation for 24 h in CO_2 incubator, old media was carefully pipetted out and subsequently, 4 ml fluorescently labelled polyplexes or lipopolyplexes (Cy5-siRNA conjugated formulations) suitably diluted in complete media was added.
- The resulting plate was incubated for 6 h protected from light in CO_2 incubator and after incubation, cells were washed three times with ice cold PBS.
- Subsequently, cells were detached using trypsin-EDTA and transferred to FACS tubes.
- This was then centrifuged at 1500 rpm for 5 min and the pellet obtained was washed with FACS buffer (1% BSA in PBS).
- After washing, the pellet was resuspended in 500 µl FACS buffer which was passed through cell strainer to remove any clumps and then subjected to analysis using fluorescence activated cell sorter (FACS-BD-AriaIII, BD, USA) to determine quantitative uptake.

6.8 Gene expression study

6.8.1 Background

Real time PCR deals with collection of data throughout PCR process and thus has capability to combine amplification and detection process in single step [21]. Currently, real time PCR is one of the most utilized technique for gene quantitation as it has several advantages including sensitivity, sequence specificity and accuracy, large dynamic range, no post-amplification processing, increased sample throughput etc [22-

24]. Real time PCR can be performed either as one step reaction where single tube is employed to perform steps of PCR from cDNA synthesis to PCR amplification, or as two step reaction where cDNA synthesis and PCR amplification are performed separately. Two types of real time quantification can be performed using qPCR – (i) Absolute quantification, where calibration curve prepared using known standard concentration is employed to determine unknown concentration [25] (ii) Relative quantification, where change in gene expression compared to reference sample is measured [26]. The detection of amplified product can be made using several detection chemistries including DNA binding dyes, hybridization probes, hydrolysis probes, hairpin probes and other fluorescent chemistries [27].

6.8.2 Protocol

6.8.2.1 Cell culture

- mRNA knockdown efficiency of the administered siRNA conjugated formulations was determined by real time PCR which quantitatively measured relative gene expression of different formulation treated SK-N-MC cells.
- The adherent cells were trypsinized and detached from tissue culture flask, and seeded at density of 1×10^6 cells/well in 6 well plate.
- After incubation for 24 h in CO_2 incubator, old media was carefully pipetted out and subsequently, the cells were treated with siRNA conjugated formulations and incubated for 48 h.
- Cells treated with PBS (pH 7.4) were used to estimate basal gene expression and the sample was employed as control.
- The cell culture thus obtained was further processed for real time PCR studies as described below.

6.8.2.2 Selection of primers

- The primers for NRG1 gene and GAPDH gene (housekeeping gene) were selected and designed using primer blast (primer designing tool) provided by NCBI (National Center for Biotechnology Information).
- The selected primers had following characteristics as described in Table 6. **1**

Table 6. 1: Characteristics of selected primers

Primer	**Sequence (5' to 3')**	**Length**	**Start position**	**Stop position**	**Tm**	**GC%**	**Self-complementarity**	**Self 3'-complementarity**
NRG1 primers								
Forward primer	AAGAGAGCGAGACAAGCCAC	20	68	87	60.04	55.00	2.00	0.00
Reverse primer	GTTTGTCCCAGGAGGGGAAG	20	262	243	59.96	60.00	4.00	0.00
Product length	195							
GAPDH primers								
Forward primer	TCTCTGCTCCTCCCTGTTCT	20	57	76	59.59	55.00	2.00	0.00
Reverse primer	GTTCACACCGACCTTCACCA	20	381	362	60.18	55.00	2.00	0.00
Product length	325							

6.8.2.3 RNA isolation

- RNA was isolated from cell culture by using TRI reagent as per manufacturer's instructions.
- For isolation, suitable volume of TRI reagent (1ml/well) was added to 6 well plate and then homogenous cell lysate was obtained by passing it through pipette.
- This was allowed to stand for 5 min at 37 °C for dissociation of nucleoprotein complexes. Later, fixed volume of chloroform (0.2 ml/ml of TRI reagent) was added and vortexed to achieve uniform mixing. This was incubated for 15 min at 37 °C.
- Later, the mixture was centrifuged at 12000 x g for 15 min at 2-8 °C which yielded 3 phases – organic phase, interphase and aqueous phase.
- RNA was present in aqueous phase and thus it was carefully separated and transferred to fresh tube and 2-propanol (0.5 ml/ml of TRI reagent) was added.
- This was vortexed and then allowed to stand for 10 min at 37 °C. The mixture was then centrifuged at 12000 x g for 10 min at 2-8 °C which gave pellet of precipitated RNA at the bottom of the tube.
- The supernatant was discarded and RNA pellet was washed by adding 70% ethanol and centrifuged at 7500 x g for 5 min at 2-8 °C.
- After centrifugation, ethanol was carefully pipetted out and RNA pellet was air dried for 5-10 min. Later, the pellet was dissolved in suitable volume of DEPC treated water.

6.8.2.4 cDNA synthesis

- cDNA was synthesized from isolated RNA by employing Hi-cDNA synthesis kit according to manufacturer's instructions.
- Before treatment, concentration of RNA solution was determined spectrophotometrically by determining optical density at λ_{max} of 260 nm and the stock solution was diluted such that final concentration of RNA solution was 1 µg/µl.
- The contents of kit were allowed to attain room temperature and then in sterile nuclease free microcentrifuge tube 5 µl 5x reaction mixture and 1 µl M-MuLV reverse transcriptase were added and mixed by vortexing.

- Later, 1 µl RNA solution (1 µg/µl) was added to above mixture and mixed properly and final reaction volume was made up to 20 µl with nuclease free water.
- The reaction mixture was incubated at 25 °C for 5 min to allow annealing of primer to RNA. This was then exposed to 42 °C temperature for 60 min which activated M-MuLV reverse transcriptase enzyme and facilitated cDNA synthesis.
- After 1 h, the enzyme was inactivated by keeping reaction mixture at 70 °C for 10 min. The cDNA thus obtained was stored at 4 °C till use.

Table 6. 2: Composition of cDNA synthesis reaction mixture

Ingredients	**Volume per reaction**
5x reaction mixture	5 µl
M-MuLV reverse transcriptase	1 µl
RNA solution (1µg/µl)	1 µl
Nuclease free water	Upto 20 µl

6.8.2.5 mRNA quantification

- 20 µl of cDNA synthesis reaction mixture prepared as mentioned in Table 6. **2** was added to MicroAmp 96 well reaction plate. This plate was sealed and then placed in QuantStudio™ 12K Flex Real- time PCR system and proceeded for analysis as per cycle mentioned below in Table 6. 3. The results obtained by RT-PCR were analyzed and % knockdown efficiency was determined.

Table 6. 3: RT-PCR cycle

Step	**Temperature**	**Duration**	**Cycles**
Enzyme activation	95 °C	180 s	Hold
Denaturation	95 °C	3 s	40
Annealing/ extension/ data acquisition	60 °C	20 s	

6.9 Result and discussion

6.9.1 Cell cytotoxicity study

PEI (25 kDa) has been reported to exhibit high cytotoxicity due to its higher surface cationic charge and less biodegradation causing accumulation toxicity [28-30]. It mainly causes two types of toxicities – (i) immediate toxicity which is caused due to

presence of free PEI which has potency to interact with negatively charged proteins and precipitate in form of clusters. This has destabilizing effect on plasma membrane and thus result in cytotoxicity. (ii) delayed toxicity which surfaces when PEI conjugated with gene therapeutics gets released from polyplexes which further interacts with cellular components causing proton leak from mitochondria and inhibition of electron transport chain which results in cell death via. apoptosis [31, 32]. All these toxicities can be circumvented by modification of PEI such that it either forms biodegradable polymer or modification results in alteration of surface charge [33].

Both these approaches were employed in this study and cytotoxicity of resulting polymers was checked using tetrazolium based MTT assay. The results of MTT assay, for synthesized copolymers and conjugates (bPEI-HA copolymer, bPEI-Lf conjugate, bPEI-Chi copolymer and biodegradable bPEI-Chi copolymer) on SK-N-MC cells, are depicted in Table 6. 4 and represented graphically in Figure 6. 3

Table 6. 4: % cell viability of synthesized copolymers and conjugates

Concentration (nmole)	**% cell viability (Mean ± SD)**			
	bPEI-HA copolymer	**bPEI-Lf conjugate**	**bPEI-Chi copolymer**	**Biodegradable bPEI-Chi copolymer**
0.1	97.72 ± 1.12	98.04 ± 1.53	97.67 ± 2.34	98.95 ± 2.42
0.5	97.24 ± 2.56	97.77 ± 2.86	98.79 ± 2.73	97.03 ± 1.49
1	96.33 ± 2.48	96.71 ± 2.09	97.99 ± 1.49	97.24 ± 2.27
5	96.39 ± 4.21	96.87 ± 1.87	96.71 ± 1.84	95.91 ± 1.45
10	96.28 ± 0.89	96.81 ± 2.82	98.15 ± 3.54	95.85 ± 3.93
50	95.11 ± 1.16	95.27 ± 1.36	96.97 ± 4.00	95.16 ± 1.54

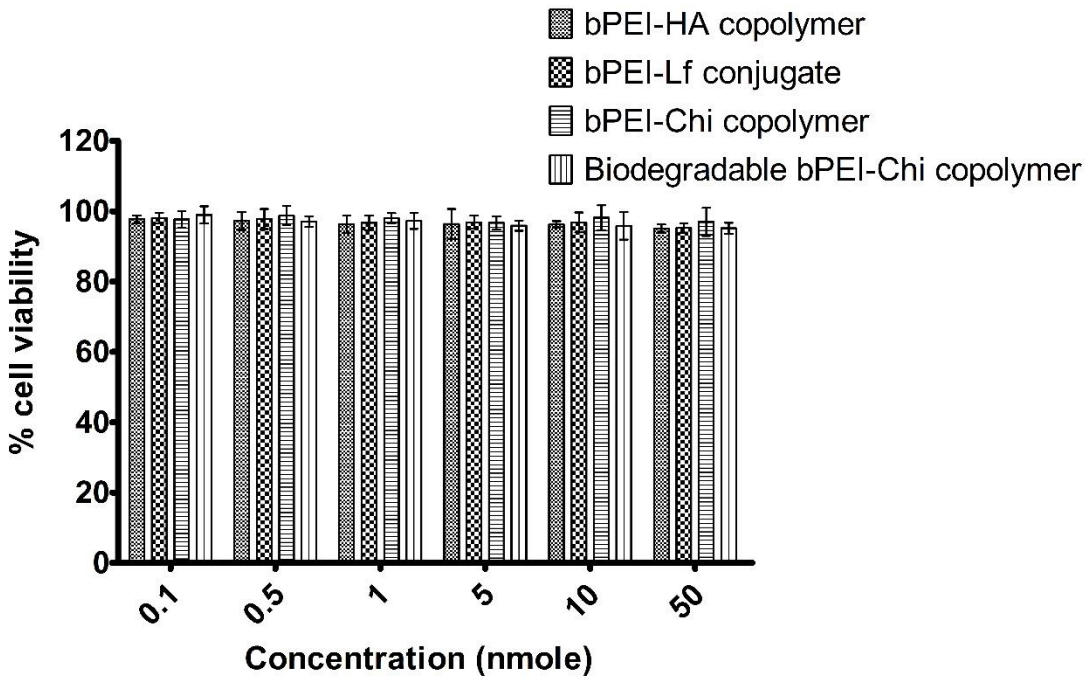

Figure 6. 3: % cell viability of synthesized copolymers and conjugates

In-vitro cell cytotoxicity study for synthesized copolymers and conjugates was evaluated thoroughly. Cytotoxicity of cells treated with saline was used as negative control. From cell cytotoxicity study, it was found that % cell viability after incubation of SK-N-MC cells with maximum concentration of bPEI-HA copolymer, bPEI-Lf conjugate, bPEI-Chi copolymer and biodegradable bPEI-Chi copolymer (i.e. 50 nmole) for 24 h was 95.11 ± 1.16, 95.27 ± 1.36, 96.97 ± 4.00, 95.16 ± 1.54, respectively. The results concluded that all the synthesized polymers exhibited negligible toxicity and thus could provide better and safe alternative for delivery of gene therapeutics to such neuronal cells. Further, in order to estimate whether enhanced safety margin of all the polymers could provide same therapeutic and transfection efficiency, quantitative and qualitative cell uptake study was performed.

6.9.2 In-vitro permeation study

The results of in-vitro permeation study using transwell is expressed as apparent permeability coefficient for all the formulations, along with enhancement ratio, in Table 6. 5. The study showed that there was significant improvement in permeability when conjugated with polyplex and lipopolyplex, resulting in improved therapeutic efficacy. This may be attributed to disruption of tight junctions integrity of cell layer. However, there was no enhancement in permeability of bPEI-HA and bPEI-Lf polyplex which

might be attributed to higher particle size and molecular weight interfering with its transfer across RPMI 2650 cells. Maximum permeability enhancement, as evident from enhancement ratio, was 3.06 for lipopolyplex which might be due to lowest particle size and enhancement of transfection efficiency [34].

Table 6. 5: Papp values of different formulations and their enhancement ratio

Formulation	Papp x 10^{-6} (cm/min)	Enhancement ratio
Naked siRNA	0.997	
bPEI-HA polyplex	0.791	0.79
bPEI-Lf polyplex	0.95	0.95
bPEI-Chi polyplex	2.47	2.48
Biodegradable bPEI-Chi polyplex	2.51	2.52
Lipopolyplex	3.05	3.06

6.9.3 Cell uptake study

6.9.3.1 Confocal microscopy

The results of qualitative cell uptake study performed employing Cy5 labelled siRNA polyplexes or lipopolyplexes and observed in confocal laser scanning microscope is represented in Figure 6. 4. The results infer that when cells incubated with naked siRNA for 6 h there was negligible fluorescence. This can be attributed to degradation of naked siRNA, large size (~ 13 kDa) and high negative charge [35]. Further, cellular uptake of polyplex and lipopolyplex increased as compared to naked siRNA, as such vectors can protect siRNA against cellular nucleases. Additionally, such vectors have resulting surface charge which may improve cellular uptake by destabilizing endosomes through proton sponge effect [36].

It was also evident that cellular uptake amongst polyplexes was dependent on particle size of them and thus bPEI-HA polyplex having particle size of 2583 nm showed lowest cellular uptake as evident from fluorescence intensity while biodegradable bPEI-Chi polyplex having particle size of 126.4 nm showed maximum uptake amongst polyplexes [37].

Finally, cellular uptake of lipoplexes conjugated with biodegradable bPEI-Chi polyplexes was found maximum amongst all siRNA conjugated vectors. This was supported by the fact that lipopolyplexes caused enhancement of clathrin mediated cellular uptake as compared to polyplexes [38].

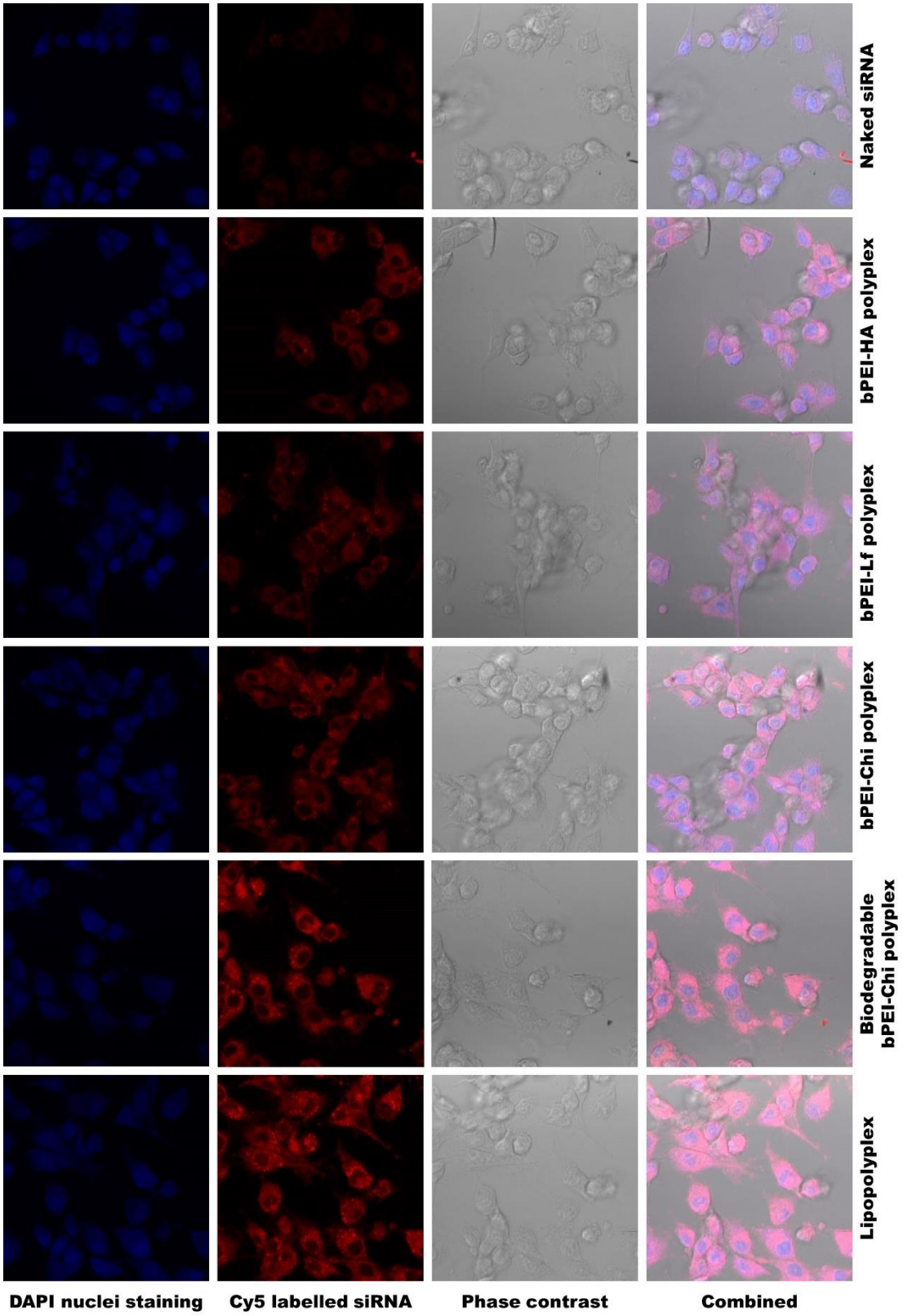

Figure 6. 4: Cell uptake study by confocal microscopy for polyplex and lipopolyplex

6.9.3.1 Flow cytometry

The results of quantitative cell uptake study are represented in Figure 6. 5.

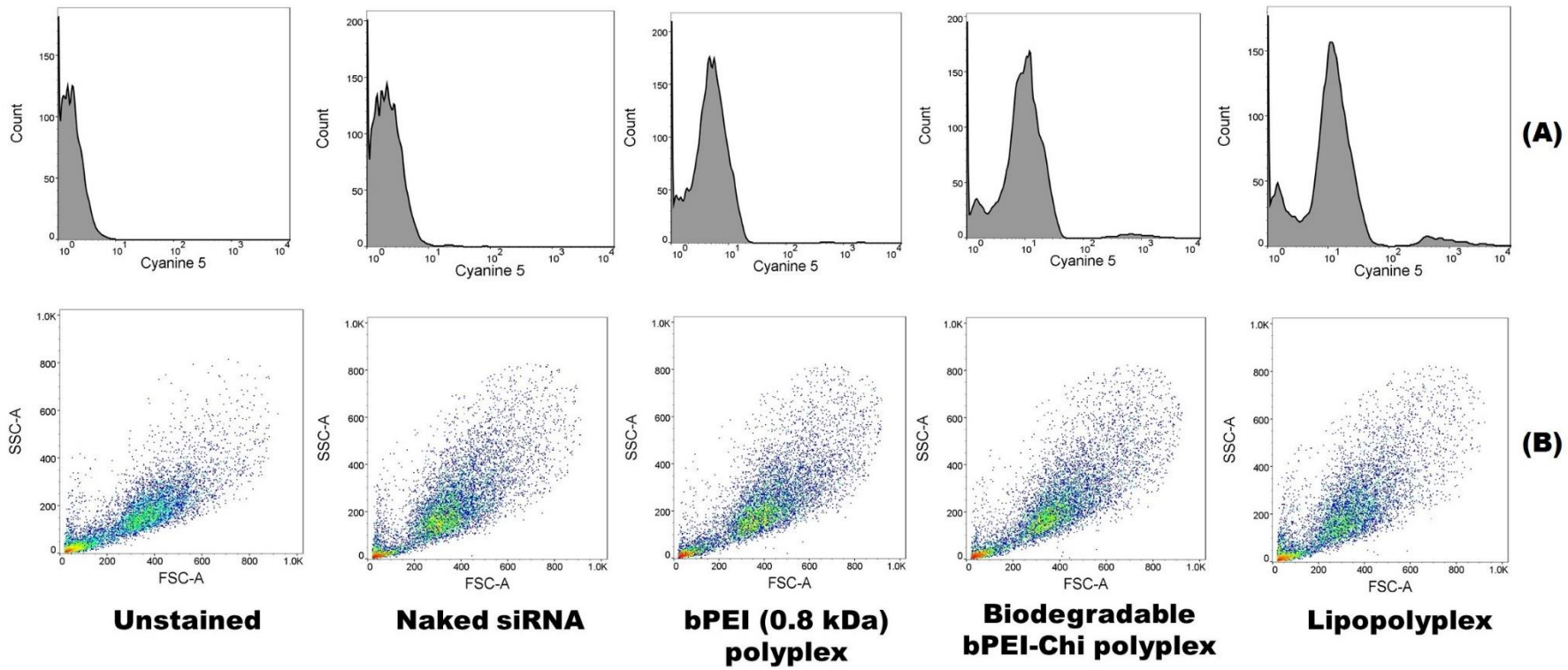

Figure 6. 5: Comparison of quantitative cell uptake of naked siRNA, bPEI (0.8 kDa) polyplex, biodegradable bPEI-Chi polyplex and lipopolyplex. (A) represents 2D histogram of population depicting Cyanine 5 positive and Cyanine 5 negative cells while (B) represents dot plots showing gated population of respective sample.

The quantitative cellular uptake of different formulations compared to naked siRNA using PEI (0.8 kDa) as control is summarized in Table 6. 6.

Table 6. 6: Summary of results of quantitative cellular uptake

Formulation	Gated population	% cells transfected	Mean Fluorescence intensity
Unstained	98.2	0.8	-
Naked siRNA	90.8	4.29	25.1
PEI (0.8 kDa)	89.6	43.1	36.7
Polyplex	88.7	71.3	55.4
Lipopolyplex	91.6	69.9	117

The results of quantitative cell uptake using flow cytometry supported the data of cellular uptake study obtained using confocal microscope. Additionally, mean fluorescence intensity of lipopolyplex was higher compared with polyplex due to enhancement of clathrin mediated cellular uptake [38], and combination of ion-pair formation and proton sponge effect for endosomal escape [39].

6.9.4 Gene expression study

The results of gene expression study performed by RT-PCR and expressed as % knockdown efficiency and relative gene expression (w.r.t. control) are depicted in Figure 6. 6 and summarized in Table 6. 7.

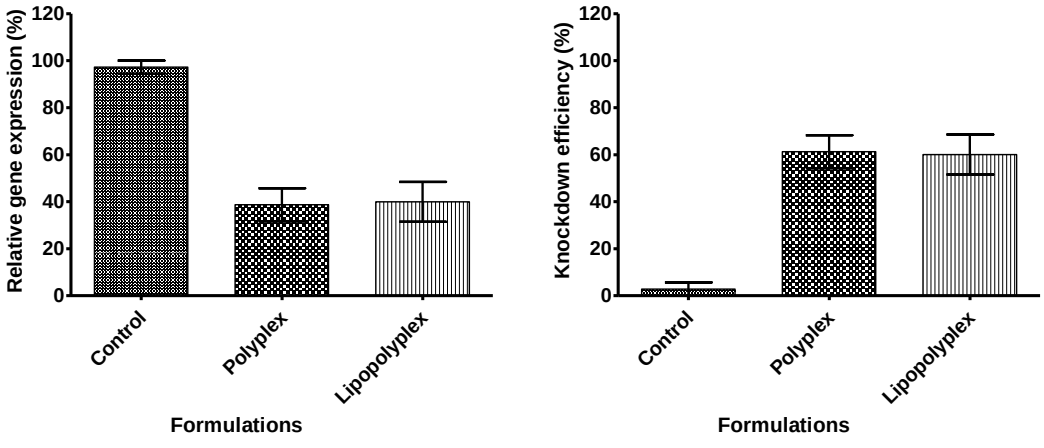

Figure 6. 6: RT-PCR analysis of polyplex and lipopolyplex

Table 6. 7: % NRG1 expression and knockdown efficiency of different treatment groups estimated by RT-PCR

Treatment	**% NRG1 expression Mean ± SD**	**Knockdown efficiency Mean ± SD**
Control	97.23 ± 2.84	2.77 ± 2.84
Biodegradable bPEI-Chi polyplex	38.72 ± 7.02	61.28 ± 7.02
Lipopolyplex	39.95 ± 8.50	60.05 ± 8.50

The results conclude that there was 38.72% and 39.95% relative gene expression when the cells were treated with NRG1 siRNA complexed polyplexes and lipopolyplexes respectively. The resultant knockdown efficiency of the treated cells was 61.28% and 60.05% respectively. The results depicted significant change in relative gene expression and thus significant knockdown efficiency when cells were exposed to treatment. This may be due to increased transfection of complexed therapeutic siRNA into the resulting cultured cells. After transfection, processing of the complexed siRNA finally leads to formation of single stranded siRNA molecules that binds to target mRNA and results in its degradation. This may be reflected as knockdown efficiency during RT-PCR [40]. Thus, this technique provides reliable and convenient method to estimate knockdown efficiency of siRNA.

6.10 References

1. *Cell line*. The American Heritage® Medical Dictionary [cited 2017 March 24]; Available from: http://medical-dictionary.thefreedictionary.com/cell+line.
2. MacDonald, C., *Development of new cell lines for animal cell biotechnology.* Crit Rev Biotechnol, 1990. **10**(2): p. 155-78.
3. Schurr, M.J., et al., *Phase I/II clinical evaluation of StrataGraft: a consistent, pathogen-free human skin substitute.* J Trauma, 2009. **66**(3): p. 866-73; discussion 873-4.
4. Gomez-Lechon, M.J., et al., *Human hepatocytes as a tool for studying toxicity and drug metabolism.* Curr Drug Metab, 2003. **4**(4): p. 292-312.
5. Kaur, G. and J.M. Dufour, *Cell lines: Valuable tools or useless artifacts.* Spermatogenesis, 2012. **2**(1): p. 1-5.
6. Mosmann, T., *Rapid colorimetric assay for cellular growth and survival: application to proliferation and cytotoxicity assays.* Journal of immunological methods, 1983. **65**(1-2): p. 55-63.
7. Van de Loosdrecht, A., et al., *A tetrazolium-based colorimetric MTT assay to quantitate human monocyte mediated cytotoxicity against leukemic cells from cell lines and patients with acute myeloid leukemia.* Journal of immunological methods, 1994. **174**(1-2): p. 311-320.
8. Vistica, D.T., et al., *Tetrazolium-based assays for cellular viability: a critical examination of selected parameters affecting formazan production.* Cancer research, 1991. **51**(10): p. 2515-2520.
9. Berridge, M.V. and A.S. Tan, *Characterization of the cellular reduction of 3-(4, 5-dimethylthiazol-2-yl)-2, 5-diphenyltetrazolium bromide (MTT): subcellular localization, substrate dependence, and involvement of mitochondrial electron transport in MTT reduction.* Archives of biochemistry and biophysics, 1993. **303**(2): p. 474-482.
10. Liu, Y., et al., *Mechanism of cellular 3-(4, 5-dimethylthiazol-2-yl)-2, 5-diphenyltetrazolium bromide (MTT) reduction.* Journal of neurochemistry, 1997. **69**(2): p. 581-593.
11. van Meerloo, J., G.J. Kaspers, and J. Cloos, *Cell sensitivity assays: the MTT assay.* Methods Mol Biol, 2011. **731**: p. 237-45.
12. Su, W., et al., *PEG/RGD-modified magnetic polymeric liposomes for controlled drug release and tumor cell targeting.* Int J Pharm, 2012. **426**(1-2): p. 170-81.

13. Li, X., et al., *Targeted delivery of doxorubicin using stealth liposomes modified with transferrin.* Int J Pharm, 2009. **373**(1-2): p. 116-23.
14. Sarmento, B., *Concepts and Models for Drug Permeability Studies: Cell and Tissue Based in Vitro Culture Models*. 2015: Woodhead Publishing.
15. Ducat, E., et al., *Cellular uptake of liposomes monitored by confocal microscopy and flow cytometry.* Journal of Drug Delivery Science and Technology, 2011. **21**(6): p. 469-477.
16. Dailey, M., et al., *Concepts in imaging and microscopy exploring biological structure and function with confocal microscopy.* The Biological bulletin, 1999. **197**(2): p. 115-122.
17. Cremer, C. and T. Cremer, *Considerations on a laser-scanning-microscope with high resolution and depth of field.* Microscopica acta, 1974: p. 31-44.
18. Ramanathan, M., *Flow cytometry applications in pharmacodynamics and drug delivery.* Pharmaceutical research, 1997. **14**(9): p. 1106-1114.
19. Cram, L.S., *Flow cytometry, an overview*, in *Advanced Flow Cytometry: Applications in Biological Research*. 2003, Springer. p. 1-9.
20. Mach, W.J., et al., *Flow cytometry and laser scanning cytometry, a comparison of techniques.* Journal of clinical monitoring and computing, 2010. **24**(4): p. 251-259.
21. Higuchi, R., et al., *Kinetic PCR analysis: real-time monitoring of DNA amplification reactions.* Biotechnology, 1993. **11**: p. 1026-1030.
22. Gentle, A., F. Anastasopoulos, and N.A. McBrien, *High-resolution semi-quantitative real-time PCR without the use of a standard curve.* Biotechniques, 2001. **31**(3): p. 502, 504-6, 508.
23. Palmer, S., et al., *New real-time reverse transcriptase-initiated PCR assay with single-copy sensitivity for human immunodeficiency virus type 1 RNA in plasma.* Journal of clinical microbiology, 2003. **41**(10): p. 4531-4536.
24. Malinen, E., et al., *Comparison of real-time PCR with SYBR Green I or 5'-nuclease assays and dot-blot hybridization with rDNA-targeted oligonucleotide probes in quantification of selected faecal bacteria.* Microbiology, 2003. **149**(1): p. 269-277.
25. Heid, C.A., et al., *Real time quantitative PCR.* Genome research, 1996. **6**(10): p. 986-994.

26. Livak, K.J. and T.D. Schmittgen, *Analysis of relative gene expression data using real-time quantitative PCR and the 2− ΔΔCT method.* methods, 2001. **25**(4): p. 402-408.
27. Wong, M.L. and J.F. Medrano, *Real-time PCR for mRNA quantitation.* Biotechniques, 2005. **39**(1): p. 75.
28. KIM, Y.-K., et al., *Degradable polyethylenimine derivatives as gene carriers.* Nano Life, 2012. **2**(01): p. 1230004.
29. Florea, B.I., et al., *Transfection efficiency and toxicity of polyethylenimine in differentiated Calu-3 and nondifferentiated COS-1 cell cultures.* The AAPS Journal, 2002. **4**(3): p. 1-11.
30. Putnam, D., et al., *Polymer-based gene delivery with low cytotoxicity by a unique balance of side-chain termini.* Proceedings of the National Academy of Sciences, 2001. **98**(3): p. 1200-1205.
31. Fischer, D., et al., *A novel non-viral vector for DNA delivery based on low molecular weight, branched polyethylenimine: effect of molecular weight on transfection efficiency and cytotoxicity.* Pharmaceutical research, 1999. **16**(8): p. 1273-1279.
32. Hall, A., et al., *High resolution respirometry analysis of polyethylenimine-mediated mitochondrial energy crisis and cellular stress: mitochondrial proton leak and inhibition of the electron transport system.* Biochimica et Biophysica Acta (BBA)-Bioenergetics, 2013. **1827**(10): p. 1213-1225.
33. Lv, H., et al., *Toxicity of cationic lipids and cationic polymers in gene delivery.* Journal of Controlled Release, 2006. **114**(1): p. 100-109.
34. Misra, A., *Challenges in delivery of therapeutic genomics and proteomics*. 2010: Elsevier.
35. Singha, K., R. Namgung, and W.J. Kim, *Polymers in Small-Interfering RNA Delivery.* Nucleic Acid Therapeutics, 2011. **21**(3): p. 133-147.
36. Boussif, O., et al., *A versatile vector for gene and oligonucleotide transfer into cells in culture and in vivo: polyethylenimine.* Proc Natl Acad Sci U S A, 1995. **92**(16): p. 7297-301.
37. Shi, J., et al., *Effect of Polyplex Morphology on Cellular Uptake, Intracellular Trafficking, and Transgene Expression.* ACS Nano, 2013. **7**(12): p. 10612-10620.

38. Schäfer, J., et al., *Liposome–polyethylenimine complexes for enhanced DNA and siRNA delivery.* Biomaterials, 2010. **31**(26): p. 6892-6900.
39. Chen, W., et al., *Lipopolyplex for Therapeutic Gene Delivery and Its Application for the Treatment of Parkinson's Disease.* Frontiers in Aging Neuroscience, 2016. **8**: p. 68.
40. Wu, W., et al., *A novel approach for evaluating the efficiency of siRNAs on protein levels in cultured cells.* Nucleic Acids Res, 2004. **32**(2): p. e17.